Two-Dimensional Melting of Alkane Monolayers Ionically Bonded to Mica

Maged A. Osman,[†] Georg Seyfang,[‡] and Ulrich W. Suter*[,†]

Department of Materials, Institute of Polymers, and Department of Chemistry, Laboratory of Physical Chemistry, ETH Center, CH-8092 Zürich, Switzerland

Received: September 27, 1999; In Final Form: February 8, 2000

The structure and phase transitions of an alkyl monolayer tethered to a mica surface have been studied by X-ray, infrared (IR) spectroscopy, and differential scanning calorimetry. All results indicate that the alkyl chains attend an all-trans conformation at low temperatures, leading to a two-dimensional crystalline film that undergoes a first-order transition to an isotropic liquid upon heating. Although the molecules are fixed to the surface at one end, which restricts their translational freedom, they undergo a melting process. It seems that the trans-gauche transformation is enough to destroy the two-dimensional lattice. A model in which the molecules assume a tilted upright position to the mica surface can explain the results obtained. To minimize the conformational entropy and maximize the packing density of the molecules, the chains attached to different mica platelets interdigitate to build an organic interlayer. A crystal−crystal transition was also observed, which led to an increase in the thickness of the organic interlayer. This increase was attributed to a change in the tilt angle of the chains to the mica surface. The phase behavior of the alkyl monolayer is quite similar to that of bulk alkanes but the transition temperatures are higher probably because of the chain end fixation. The solid−liquid transition influenced the IR spectrum but not the film thickness, whereas the solid−solid transition did the contrary. However, both phase transitions were observed in the differential scanning calorimetry. It was possible to differentiate between bonded and intercalated molecules by thermogravimetric analysis, because their decomposition temperatures were different.

Introduction

Upon melting, the molecules of conventional crystalline solids [three-dimensional (3D) order] undergo a large and simultaneous change in rotational, positional, and orientational order. In contrast, anisometric rigid rodlike molecules often lose their order stepwise, giving rise to mesophases. An initial breakdown leads to rapid oscillation or rotation about the long molecular axis, which is followed by a collapse of the long-range positional order. The local packing is then destroyed, whereas the long-range orientational order is largely retained. Finally, disruption of the long-range order takes place, leading to a completely disordered liquid.[1] Flexible rodlike molecules, such as acyclic n-alkanes, show crystalline phases, some of which are transformed on heating into a less dense rotator solid (α) phase before they melt to an isotropic liquid.[2−4] Thermotropic liquid crystalline phases are unlikely to be observed in such alkanes, because the energy difference between the trans and gauche conformers is small. This leads to an early loss of the anisometry of the all-trans conformer and hence the long-range orientation collapses before the long-range positional order. Thermotropic phase transitions have also been observed in amphiphilic alkyl molecules−water systems.[5−8]

Ultrathin films (monolayers) of flexible rodlike molecules (liquid or solid supported), which by definition can only have two-dimensional (2D) order at maximum, if any, have been studied for years.[9] Phase transitions were observed in these films and they continue to attract a great deal of interest.[10,11] Nowadays, it is generally accepted that thermal first-order phase transitions occur in Gibbs and Langmuir monolayers.[12,13] The condensed monolayer at the water−air interface is a result of the equilibrium between the attractive forces, driving the molecules together, and the entropy, which tends to disperse them. In these films, the substrate does not exert any limitation on the molecular order.

Short n-alkanes have been physisorbed on metal surfaces and were found to build ordered ultrathin overlayers that undergo thermal phase transitions.[14−16] To optimize the weak interaction between the adsorbate and the substrate in the ordered phase, the alkyl chains lie with the planes of the all-trans carbon backbones parallel to the metal surface and form a well-defined 2D lattice. The melting temperatures of the investigated alkane films, measured by infrared (IR) spectroscopy, were quite similar to those measured by differential scanning calorimetry (DSC) in bulk. 2D crystalline phases were also observed in self-assembled monolayers of long alkyl thiols on metal surfaces.[17−20] In this case, the densely packed alkyl chains assume an upright position to the surface, due to the strong interaction of sulfur with metals, with a tilt angle that depends on the type of the substrate. The thermodynamic stability of these 2D crystalline phases has been the subject of a dispute and it is not clear how the melting temperatures of the alkyl thiol monolayers compare with those of the corresponding 3D crystals.[21,22] Self-assembled monolayers of alkanoic acids were also formed on metal surfaces and their structures studied.[23−26] Long alkyl chains were found to densely pack to give well-organized 2D lattices similar to those of the thiols, but the phase transitions in these films were not investigated. The structure of such ultrathin films are not only influenced by the interaction between the alkyl chains, but also by the binding geometry of the headgroups. The metal

[†] Department of Materials.
[‡] Department of Chemistry.
* Phone: +41 1 6323127; fax: +41 1 6321096; e-mail: suter@ifp.mat.ethz.ch.

10.1021/jp993448z CCC: $19.00
Published on Web 04/07/2000

surfaces used in those investigations have the advantage of being uniform and of not exerting any space limitation on the packing of the assembled molecules.

Layered aluminosilicates, despite their constitutional heterogeneity, are scientifically and technologically interesting substrates to which organic molecules can be ionically bonded by exchange reactions.[27,28] In contrast to metal surfaces, the organic cations bind only to the negatively charged sites of the aluminosilicates, which are limited in number and differ in density from one mineral to the other. Therefore, it is not self-evident that flexible rodlike molecules bonded to these surfaces can densely pack into ordered lattices. The exchange also occurs on the free surface of the aluminosilicate platelets dispersed in aqueous media. In the dry state, where the platelets are aggregated, it is an open question whether the hydrophobic organic monolayers should be regarded as overlayers or as soft condensed matter confined between two hard walls. Extended X-ray diffraction (XRD) studies on ultrathin alkylammonium films formed on clay mineral surfaces have been carried out by Weiss[29,30] and Lagaly.[30−33] From basal-plane spacing measurements, these authors concluded that long alkyl chains assume an upright position to the surface and are ordered. Lagaly also pointed out that the alkyl chains in these monolayers tend to include unreacted molecules and it is necessary to extensively wash the organosilicates. He intercalated alkyl alcohols between the alkylammonium cations bonded to beidellite to obtain densely packed bimolecular films, the thickness of which were temperature dependent. This temperature dependence was attributed to the formation of kink-block and gauche-block structures on heating. However, no phase transitions were reported for the monomolecular alkylammonium monolayers. Giannelis and co-workers[34] studied the structure of alkyl- and dialkylammonium films formed on different montmorollinites by XRD, IR, and DSC and were able to show that the alkyl chains assumed an ordered state. Thermotropic phase transitions were also observed in these films. The authors postulated molecular arrangements varying from solidlike to liquidlike and in intermediate cases liquid−crystalline, depending on the packing density and chain length. However, it is not clear how a monolayer of alkyl chains with fixed ends can adopt a liquid crystalline order. Also, different clay minerals with varying exchange capacities were used as substrates to elucidate the influence of the packing density on the structure of the organic film, although the packing density is not only influenced by the total charge density, but also by the charge distribution. Since the charge distribution in the layers of smectites is inhomogeneous and differs from one clay mineral to the other, the distribution of the alkyl chains bonded to different aluminosilicates will differ and consequently so will their packing density.[28,35,36]

Muscovite mica is a 2:1 layered silicate and its crystal structure consists of two tetrahedral silica sheets sandwiching an octahedral alumina sheet. On average one silicon atom of four is replaced by aluminum, giving rise to localized negative surface charges that are more homogeneously distributed than those of montmorillonite. Therefore, muscovite is better suited to serve as substrate for such studies. Unfortunately, its cation exchange capacity (CEC) is two orders of magnitude lower than that of montmorillonite because it does not swell and its interlayer cations are not exchangeable under ambient conditions. The low concentration of the exchanged organic molecules on the surface hinders the investigation of their structures. In previous studies, it was shown that partially delaminated muscovite has high specific surface area and therefore can be used to study the exchange reactions of organic molecules.[37−40] Here, monolayers of octadecyltrimethylammonium cations have been bonded to such partially delaminated muscovite mica surfaces, and the structure and phase behavior of these films were investigated by IR, XRD, and thermal analysis.

Experimental Section

Reagents. Octadecyltrimethylammonium chloride (ODTA), purum (Fluka, Buchs, Switzerland), and pro-analysi grade chemicals (Merck, Darmstadt, Germany) were used without further purification. Millipore Ultrapure water (pH 5.8, G 1 μS/cm) was also used in all experiments.

Li−Mica. A partially delaminated muscovite (CEC = 460 μeq/g, surface area = 130 m^2/g) with a surface saturated with lithium ions was prepared by treating mica fines (a waste product of mica paper manufacture, supplied by von Roll Isola, Breitenbach, Switzerland) with hot saturated lithium nitrate solution. The delamination procedure was previously described.[38] The same batch of delaminated mica was used in all experiments.

Exchange Isotherm. Fifty milligrams of Li−mica, the corresponding amount of a 5 mmol/L ODTA solution, and the necessary amount of water to fill up to 25 g were shaken in polypropylene (PP) vials at room temperature. After 7 h, the vials were centrifuged and the supernatant liquid filtered through a cellulose acetate filter with 0.45 μm pore diameter (Schleicher and Schuell, Dassel, Germany). The first 2 mL of the filtrate was discarded and the remainder was analyzed. The Li^+ concentration was determined by inductively coupled plasma−optical emission spectrometry (ARL 3580 B, Appl. Res. Lab. SA, Ecublens, Switzerland).

ODTA−Mica. The lithium surface ions of the delaminated mica were exchanged for $ODTA^+$ by dispersing 1 g of Li−mica in 70 mL of water and 15 mL of methanol through stirring and sonication. To this dispersion, the required amount of ODTA, dissolved in 15 mL of methanol, was slowly added under stirring and the mixture was stirred for 2 h. The suspension was then centrifuged in a PP tube, and the mica washed by shaking with methanol−water mixture (1:2) for 1 h. Finally, the mica was washed with methanol, centrifuged, and dried at 70 °C under reduced pressure.

Thermal Analysis. The thermogravimetric analysis (TGA) was carried out in air at a heating rate of 20 °C/min on a TGA 7, whereas the DSC was carried out at a rate of 10 °C/min on a DSC 7 (Perkin-Elmer, Norwalk, CT).

IR-Spectroscopy. IR transmission spectra were collected using a grating double-beam spectrometer PE 983 (Perkin-Elmer) operating at 6 cm^{-1} resolution with an unpolarized beam striking the powder sample held between CaF_2 windows at normal incidence. The spectrometer was calibrated with an accuracy of $\pm$0.2 cm^{-1} against HCl frequencies taken from IR standards. For resolution-limited detectors, the precision with which a line position can be measured is determined by the reliability of the frequency calibration and the ratio of the spectral resolution ($\Delta\nu$) divided by the signal-to-noise ratio (S/N). Because the measured spectra showed a half-width (full width at half-maximum) of 15−25 cm^{-1} (significantly larger than the spectral resolution used), the precision is determined only by S/N. Therefore, a spectral resolution of 6 cm^{-1} was chosen to improve S/N. Measurements made with a resolution of 2−3 cm^{-1} on the PE 983 instrument as well as those made with a resolution of 0.5 cm^{-1} on a Bruker IFS 66-V Fourter transformed (FT) IR spectrometer did not show any significant difference. A temperature-controlled cell and a Fenwal controller

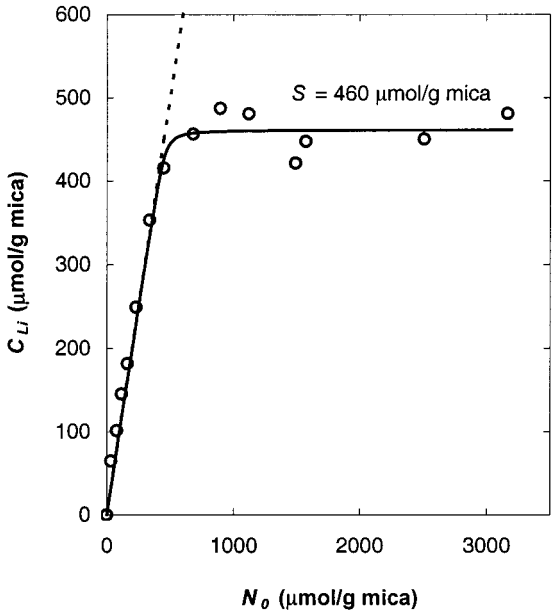

Figure 1. Dependence of equilibrium Li^+ release (C_{Li}) on initial amount of $ODTA^+$ (N_0) in the system. The solid line is a fit calculated by nonlinear regression according to eq 1; the dashed line represents quantitative exchange.

ser. 550 were used to thermostat the sample (Fenwal, Ashland, MA). The cell was heated to the desired temperature and kept there for at least 10 min so that the sample could attain this temperature before the spectrum was recorded. The temperature of the cell body was registered by an additional thermocouple.

X-Ray Diffraction. Wide-angle diffraction patterns (WAXRD) from powder samples filled in 0.5-mm glass capillaries were obtained in transmission mode at different temperatures on a Stoe Stadi powder diffractometer using Cu−Kα (0.15406 nm) radiation (45 mA, 45 kV). The diffractometer was equipped with a heating chamber, a curved Ge (111) primary beam monochromator, and a linear position-sensitive detector (PSD). The data collection for an oriented sample was performed in reflection mode on a Philips PW1820-APD 1700 powder diffractometer with monochromatized Cu−Kα radiation. The instrument was equipped with a graphite monochromator and a proportional xenon detector.

Results

Exchange Isotherm. The exchange equilibrium was studied by exposing Li−mica to different amounts of ODTA. Although the $ODTA^+$/ Li^+ exchange was expected to be fast because all other reported Li^+ exchange reactions with organic and inorganic cations had been completed within 1 h, the reaction time was prolonged to 7 h to ensure that equilibrium was reached.[37,39,41,42] The amount of released Li^+, which is equivalent to that of $ODTA^+$ adsorbed, was measured and plotted against the initial amount of organic cation introduced into the system (Figure 1). It can be seen that the amount of released Li^+ increased with increasing initial amount of $ODTA^+$/g mica until a final saturation value was reached. This behavior was expected from an ion-exchange reaction on a surface with fixed number of charges. The exchange equilibrium K can be described by

$$K = \frac{C_{\mathrm{Li}}^{\ 2}}{(N_0 - C_{\mathrm{Li}})(S - C_{\mathrm{Li}})} \qquad (1)$$

where N_0 is the initial amount of $ODTA^+$ in μmol/g mica, S is the CEC in μmol/g mica, and C_{Li} is the amount of released Li^+ in μmol/g mica.[37] K and S can then be calculated by nonlinear regression, and the regression curve is shown in Figure 1 as a solid line. The S value was found to be 460 μmol/g mica, which is comparable with the value (450 μmol/g mica) obtained from the Li^+/alkali metal ions exchange.[41] The K value was too high (over 20) to be accurately determined, reflecting the high affinity of the alkylammonium cation for mica.

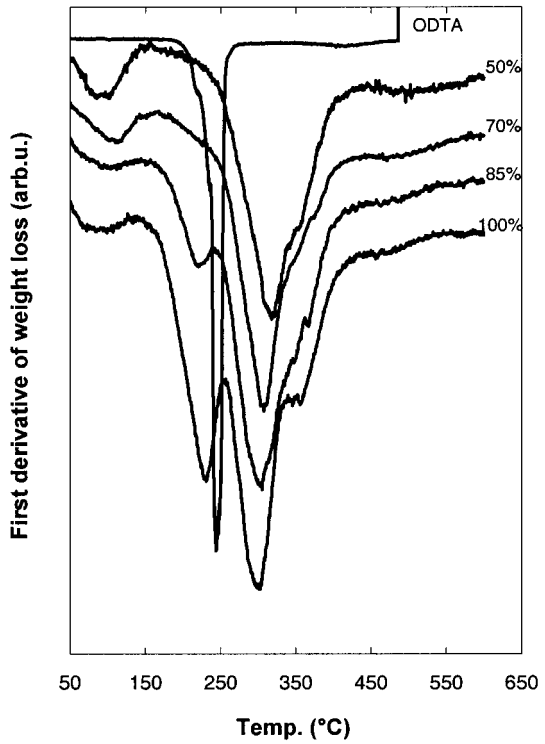

Figure 2. Change in the decomposition rate of ODTA−mica with different surface coverage (in percentage of the CEC) on heating.

Thermal Analysis. TGA of ODTA−mica showed that up to 900 °C, the organic layer did not burn completely either in air or in pure oxygen atmosphere, and the remaining mica became dark in color. Mica [ideal formula $K_2Al_4(Al_2Si_6O_{20})(OH)_4$] also gradually dehydrated (mainly above 450 °C), so that the amount of adsorbed ODTA could not be quantitatively determined by TGA. However, the weight loss between 150 and 440 °C gave a good estimate of the amount of ODTA present in the sample. The weight loss below 150 °C was due to the desorption of water adsorbed on the surface. Figure 2 shows the change in the decomposition rate with temperature (first derivative of weight loss) of ODTA−mica samples exchanged to different degrees as well as that of ODTA itself. Obviously, the $ODTA^+$ bonded to mica is more thermally stable than the bulk material, and a two-step weight loss, manifesting itself in the first derivative curve by two peaks (rate maxima), indicates the presence of unbonded molecules. ODTA−mica with 50% and 70% surface coverage showed only one peak, whereas the samples reacted with ODTA amounting to 85% and 100% of the CEC showed two peaks. Upon further washing of the 85% sample, the peak below 250 °C in Figure 2 disappeared, showing that this part of the ODTA is not chemically bound to the mica surface. This was done in PP vials to avoid contamination with the ions ubiquitous on glass surfaces, which may reexchange the $ODTA^+$. The lower decomposition temperature of the unbonded ODTA versus the bulk material indicates that the molecules are intercalated and arrange themselves in an antiparallel fashion to the bonded ones,

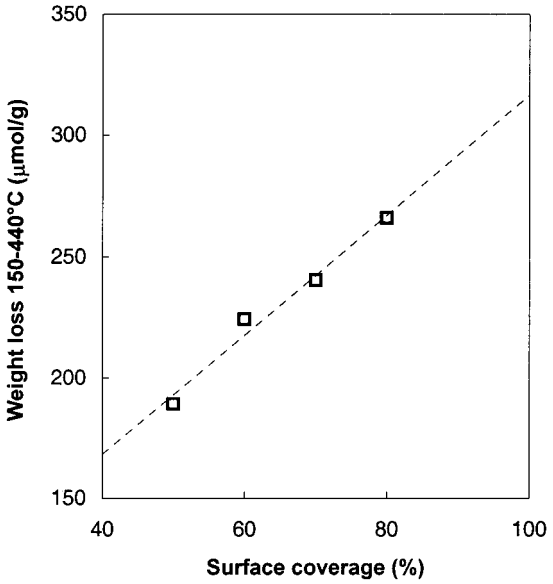

Figure 3. Weight loss of ODTA−mica on heating as a function of surface coverage.

in which case the more oxidation-sensitive amino groups of the intercalated molecules are exposed to the air. Washing out of the intercalated ODTA in samples reacted with 100% or more of the CEC needed several shakings with methanol for long periods of time, and it was not possible to completely get rid of it. Figure 3 shows a plot of the weight loss on heating of ODTA−mica with different amounts of surface coverage, expressed in μmol of $ODTA^+$/g, against the amount of ODTA introduced into the reaction, expressed in percent of the CEC. A linear relation for the decomposition of bonded ODTA was found, which gives a loss of 316 μmol of $ODTA^+$/g upon extrapolation to 100% surface coverage. This value is 30% lower than the CEC calculated from the reaction isotherm shown in Figure 1, in accordance with the observation reported above that the bonded ODTA does not burn completely. An attempt to measure the weight loss of similarly exchanged undelaminated mica was made but failed because of the insufficient sensitivity of the instrument.

The calorimetric behavior of ODTA monolayers bonded to mica, the concentration of which varied between 50 and 80% of the CEC, was scanned between −25 and 120 °C at a rate of 10 °C/min. Irrespective of the degree of exchange, all samples showed two endothermic peaks at 43 and 69 °C on heating. A metastable modification was formed on cooling the 80% sample, which had a transition temperature at 52 °C (Figure 4). For the samples with 50−70% surface coverage, no phase transition was observed on cooling. However, in all cases the phase transitions could be observed again on heating after cooling the samples for several hours at room temperature. The transition enthalpies (ΔH) were proportional to the surface coverage but also depended on the history of the sample. The longer the sample stood at room temperature, the higher ΔH was. This hindered an accurate determination of ΔH, however values up to 12 kJ/mol $ODTA^+$ were obtained for the transition at higher temperature. The presence of intercalated ODTA had little influence on the transition temperatures but increased ΔH. An attempt to measure the transition temperatures in an undelaminated ODTA−mica sample failed because of the low concentration of ODTA bonded to the surface.

IR Spectroscopy. The high-frequency absorption spectra of nonadecane in the crystalline and isotropic states are plotted in Figure 5. At 25 °C, four distinct peaks were observed at 2848,

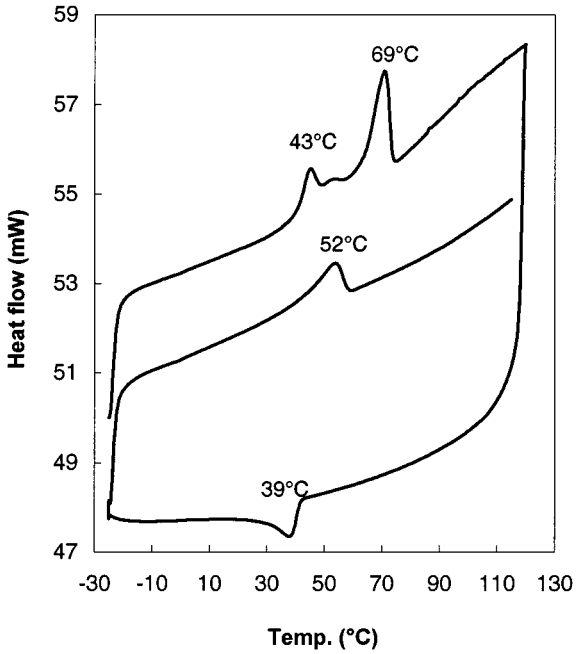

Figure 4. DSC trace of partially delaminated mica, in which 80% of the surface cations were exchanged with $ODTA^+$.

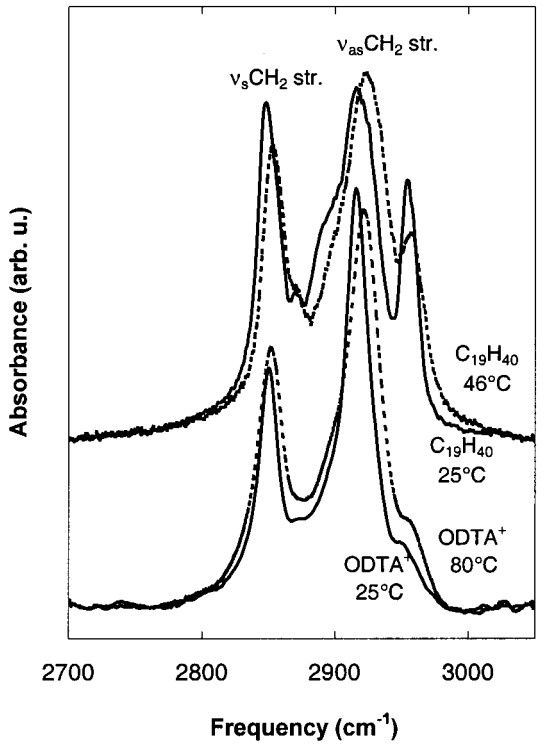

Figure 5. High-frequency IR spectra of nonadecane and ODTA mica (80%) below and above the transition temperature.

2870, 2916, and 2955 cm^{-1}, which were straightforwardly assigned to the CH_2 symmetric, CH_3 symmetric, CH_2 antisymmetric, and CH_3 asymmetric stretching C−H vibrations, respectively.[43−47] The positions of the CH_2 mode peaks correspond to the high trans conformational populations of the alkyl chains in the crystalline phase. In the melt at 46 °C, the CH_2 stretching bands were shifted to 2853 and 2923 cm^{-1} respectively, reflecting the temperature-dependent changes in the conformation of the alkyl chains. Nonadecane is known to adopt an orthorhombic crystal structure below 22°C, in which the chain rotation is greatly restricted and the chains are perpendicular to

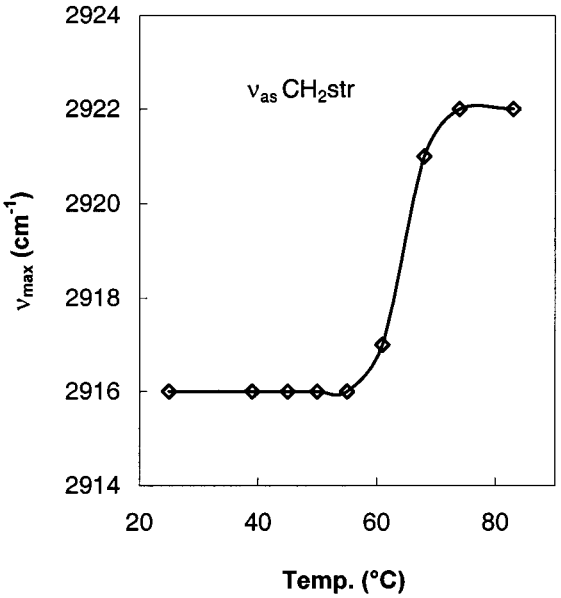

Figure 6. Temperature dependence of the antisymmetric CH_2 stretching vibration frequency of 80% ODTA mica.

the end group planes. Above this temperature the crystals are transformed into a hexagonal form, in which the molecules rotate about the long chain axes.[2,3] No difference in the high-frequency IR spectrum could be observed below and above 22 °C. Octadecane, which has a triclinic crystal structure with the alkyl chains tilted 73° to the end group planes, showed the same spectra as nonadecane below and above the melting point. In other words, the crystal form did not influence the frequency of the absorption bands, but the change in chain conformation and environment upon melting did.

The IR spectra of ODTA−mica with 80% surface coverage at 25 and 80 °C are also shown in Figure 5. They show distinct frequency shifts from 2850 to 2853 cm^{-1} for the methylene C−H symmetric stretching band and from 2916 to 2922 cm^{-1} for the methylene C−H antisymmetric stretching band. The temperature dependence of the methylene C−H asymmetric stretching vibration is plotted in Figure 6, showing that the transition to the isotropic state occurs at ca. 65 °C, that is, at the second transition temperature observed by DSC. The observed frequency shifts with temperature were reversible. Samples with different degrees of surface coverage (50−80%) as well as samples containing intercalated ODTA all showed exactly the same behavior.

X-ray Diffraction. The WAXRD patterns of ODTA−mica with 80% surface coverage were measured in the temperature range 30−80 °C, at 5 °C intervals, and the reflections in the 2θ range of 4−11° are recorded in Figure 7. Because the mica was only partially delaminated, the 001 basal reflection of muscovite could be recorded and was taken as an internal standard. From the diffraction pattern of an oriented sample recorded down to $2\theta = 2°$, which showed the lower-order basal reflections, the 30 °C peak at 6.81° could be assigned to the 003 basal plane of ODTA-mica. This peak was found to broaden and to shift down to 6.57° at 80 °C. Applying Bragg's law, $d = \lambda/(2\sin\theta)$ with $\lambda = 0.15406$ nm, an increase in the basal-plane spacing from 3.96 to 4.31 nm can be calculated. The temperature dependence of the basal-plane spacing is plotted in Figure 8, showing that the increase in spacing occurs at ca. 47 °C, which corresponds approximately to the first transition temperature observed by DSC. At higher temperatures, no appreciable increase in the basal-plane spacing could be measured. Since the dimensions

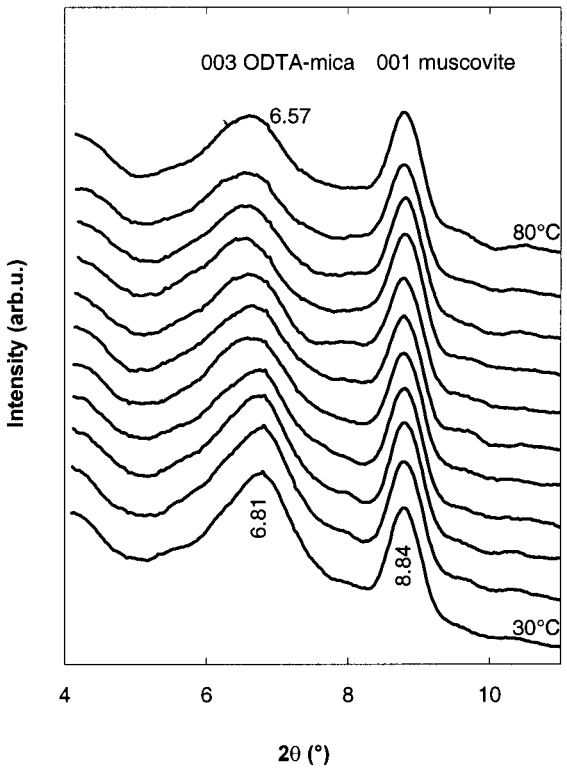

Figure 7. Transmission XRD patterns of partially delaminated mica, in which 80% of the surface cations were exchanged with $ODTA^+$, in the temperature range of 30−80 °C.

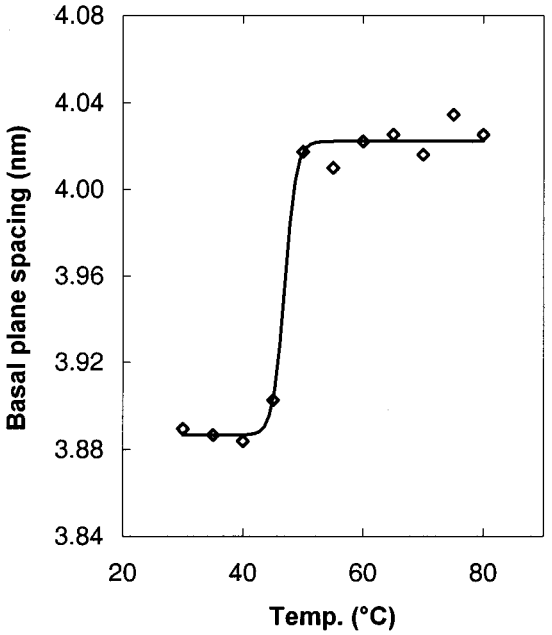

Figure 8. Temperature dependence of the basal-plane spacing of 80% ODTA−mica.

of the silicate sheets remain constant in this temperature range (to better than 1%, which is within the accuracy of the measurements), the organic film thickness can be estimated from the basal-plane spacing by deducting the thickness of the silicate layer (1 nm). Hence, the thickness of the ODTA film at 30 °C is 2.96 nm and increases to 3.31 nm above the first transition temperature observed by DSC. The WAXRD curves of ODTA-mica samples with different surface coverage, collected at 30 and 80 °C, are plotted in Figure 9. It was not possible to accurately determine the peak position of the 50% sample because it was too broad. Both samples with 70 and 80% surface

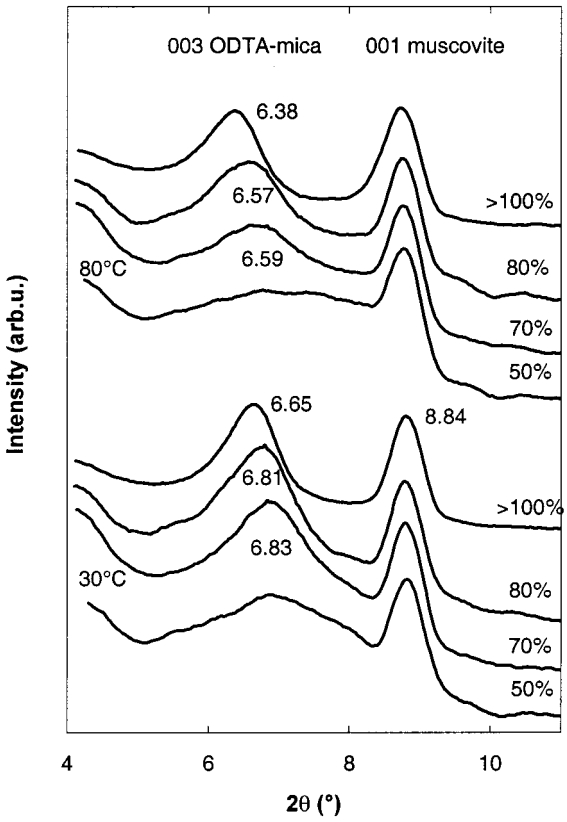

Figure 9. Transmission XRD patterns of ODTA−mica with different surface coverage below and above the transition temperature.

coverage showed identical patterns at 30 and 80 °C; however, the presence of unbonded ODTA (>100% surface coverage) increased in the basal-plane spacing by 0.03−0.09 nm. In other words, a surface coverage of 70−80% gave the ultimate thickness of the ODTA monolayer, whereas the presence of intercalated molecules lead to ca. 4% increase in the layer thickness.

Discussion

From the reaction isotherm (Figure 1), it can be seen that the $ODTA^+/Li^+$ exchange was quantitative up to ca. 80% of the CEC. Above this value the isotherm deviates slightly from the dashed line with slope 1, which represents quantitative exchange. From eq 1, K is infinite when C_{Li} equals N_0 and decreases asymptotically upon deviation from quantitative exchange. Therefore, K is high (over 20) and cannot be accurately determined. Because K is a measure of the relative affinities, it can be concluded that the affinity of $ODTA^+$ for mica is much higher than that of Li^+.

Because the goal of this study is to investigate the structure and phase behavior of n-alkane monolayers, it is necessary to ensure that only chemically bonded ODTA is present on the mica surface. In other words, bilayers and multilayers, that is, intercalated molecules and bulk material, have to be avoided. This problem led investigators of organoclays to tedious washing procedures without having an analytical tool to control the purity of the prepared samples.[36] As can be seen from Figure 2, TGA is a suitable method for detecting both bonded and unbonded material, provided that the surface area of the mineral is high enough, that is, the concentration of the organic molecules is higher than the sensitivity limit of the instrument. In case of the partially delaminated mica, this condition is fulfilled.

IR spectroscopy has proven to be a powerful tool in investigating the structure of 3D as well as 2D lattices of alkanes on a microscopic level.[15,17,20,34,45−50] The C−H stretching frequencies were found to be significantly affected by the conformational changes in the alkyl chains and the lateral chain−chain interactions. Shifts to higher frequencies were observed upon melting the alkanes, that is, on going from the crystalline all-trans conformation to a disordered state. For instance, the methylene C−H asymmetric stretching band was shifted 8 cm^{-1} higher. Because reflection IR measurements for nonmetallic surfaces such as that of mica are hindered by the low reflectivity, the thin delaminated mica platelets were used in transmission. This also helps the problem that the absorbance of mica and the interference fringes from the parallel surfaces of $>1\mu$m-thick mica plates obscure the weak absorbance of the ultrathin films in FTIR.[51] The high surface area of the thin mica platelets also leads to a higher concentration of the organic molecules. As shown in Figure 5, the methylene C−H asymmetric stretching band of the ODTA monolayer at room temperature has the same frequency as that of crystalline nonadecane, emphasizing the high degree of order in the alkyl chains in this film. At 65 °C, the absorption frequency is shifted 7 cm^{-1} higher (Figure 6), indicating a transition to a disordered liquid state. This phase transition corresponds to the second transition observed by DSC. The frequency of the symmetric stretching at room temperature is 2 cm^{-1} higher than that of crystalline nonadecane but is shifted to the same value as that of liquid nonadecane upon heating. The striking similarities between the spectra of crystalline nonadecane and ODTA mica as well as their akin thermal behavior strongly suggest that a solid−liquid phase transition takes place in the ODTA film at the second transition temperature. The fact that above this transition temperature the frequencies of both absorption bands are identical to those of liquid nonadecane indicates that the ODTA film is in an isotropic state. No frequency shifts were observed between 20 and 60 °C, that is, across the first transition temperature measured by DSC, which suggests that this might be a transition from one crystal form to another without essential change in the conformation of the alkyl chains.

The DSC trace (Figure 4) shows clearly that a first-order transition occurs at the same temperature (69 °C) as the IR frequency shifts, supporting the hypothesis that these shifts are due to a melting process. The observed supercooling and the history dependence of ΔH also indicate that a slow crystallization process takes place on cooling. The formation of a metastable modification also supports a crystal−liquid transition. At 43 °C, another phase transition with smaller ΔH was observed, which had no influence on the IR spectrum. This behavior is quite similar to that of nonadecane, but the transition temperatures are 20 and 35 °C, respectively, higher than those of nonadecane, probably due to the tethering of the alkyl chain ends to the mica surface, which restricts their translational freedom.

The X-ray measurements (Figure 7) show that the basal-plane spacing of the silicate layers has been widened by the ODTA molecules and that the thickness of this film at 30 °C is 2.96 nm. This is larger than the length (2.6 nm) of a fully extended ODTA molecule (dioctadecyl dimethylammonium = 2.6 nm, nonadecane = 2.62 nm).[2,34] Since the IR spectrum shows that at ambient temperature the alkyl chains adopt an all-trans conformation, it can be expected that the chain length will slightly decrease upon heating because of the increase in the gauche populations. This should lead to a slight decrease in the basal-plane spacing. However, the contrary occurs and the basal-plane spacing increases by 0.35 nm at 47 °C, which corresponds to the first transition observed by DSC. Also, the cross-sectional

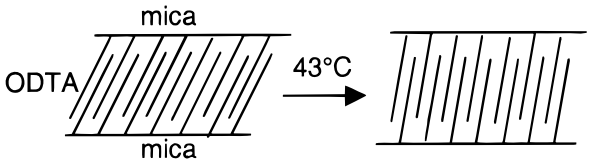

Figure 10. Schematic representation of the solid−solid phase transition.

area of an extended alkyl chain is ca. 0.2 nm^2, whereas the available area per cation on muscovite is 0.47 nm^2.[52] In other words, the chains have more than twice as much space available as that needed for a close packing in a crystalline lattice. However, both IR and DSC measurements show that the ODTA film is crystalline at low temperatures. To cope with these facts, we suggest that the ODTA molecules attend an upright but tilted position to the surface with the chains attached to two mica platelets interdigitating and partially overlapping to minimize their conformational entropy, and assume a thermodynamically favorable dense packing (Figure 10). At 43 °C, a transition to another crystal modification, in which the chains adopt a larger angle to the surface, takes place and the basal-plane spacing increases (but no frequency shift in the IR spectrum).

The melting of the crystal lattice at the second transition temperature seems to have no appreciable influence on the basal-plane spacing, whereas it causes frequency shifts in the IR spectrum. The fact that a melting process (crystalline-isotropic) takes place in these films, although the molecules have limited translational freedom because of their end fixation to the surface, is somewhat surprising. However, it seems that the trans-gauche transformation is enough to destroy the 2D order of the chains. Actually the cation exchange occurs in aqueous media on the surface of the dispersed Li−mica platelets, but on flocculation the external surfaces are turned into internal ones. This process can be reversed by redispersion in an appropriate liquid.

Conclusion

The alkyl ultrathin films, ionically bonded to mica, crystallize at low temperatures and can have different crystalline modifications. Upon heating, the crystal lattice is destroyed because of an increase in the gauche populations, leading to an isotropic liquid. This behavior is quite similar to that of bulk alkanes; however, the transition temperatures in the alkyl monolayer are higher, which might be attributed to the restricted translational freedom of the surface-bound chains.

Acknowledgment. We gratefully acknowledge financial support from the Swiss Commission for Technology and Innovation (CTI).

References and Notes

(1) Goodby, J. W. In *Handbook of Liquid Crystals*; Demus, D., Goodby, J. W., Gray, G. W., Spiess, H. W., Vill, V., Eds.; Wiley-VCH: Weinheim, 1998; Vol. 2A, p 3.
(2) Broadhurst, M. G. *J. Res. Natl. Bur. Stand.* (*U.S.*) **1962**, *66A* , 241.
(3) Turner, W. R. *Ind. Eng. Chem. Prod. Res. Dev.* **1971**, *10*, 238.
(4) McClure, D. W. *J. Chem. Phys.* **1968**, *49*, 1830.
(5) Cameron, D. G.; Umemura, J.; Wong, P. T.; Mantsch, H. H. *Colloids Surf.* **1982**, *4*, 131.
(6) Kawai, T.; Umemura, J.; Takenaka, T.; Kodama, M.; Seki, S. *J. Colloid Interface Sci.* **1985**, *103*, 56.
(7) *Micelles, Membranes, Microemulsions and Monolayers*; Gelbart, W. M., Ben-Shaul, A., Roux, D., Eds.; Springer: Heidelberg, 1994.
(8) Als-Nielsen, J.; Kjaer, K. In *Phase Transitions in Soft Condensed Matter*; Riste, T., Sherrington, D., Eds; NATO ASI Series B; Plenum: New York, 1989.
(9) Ulman, A. *An Introduction to Ultrathin Organic Films*; Academic Press: San Diego, 1991.
(10) *Phase Transitions in Surface Films*; Dash, J. G., Ruvalds, J., Eds.; Plenum: New York, 1980.
(11) Naselli, C.; Rabolt, J. F.; Swalen, J. D. *J. Chem. Phys.* **1985**, *82*, 2136.
(12) Barton, S. W.; Thomas, B. N.; Flom, E. B.; Rice, S. A.; Lin, B.; Peng, J. B.; Ketterson, J. B.; Dutta, P. *J. Chem. Phys.* **1988**, *89*, 2257.
(13) Vollhardt, D. *Adv. Colloid Interface Sci.* **1999**, *79*, 19.
(14) Hostetler, M. J.; Manner, W. L.; Nuzzo, R. G.; Girolami, G. S. *J. Phys. Chem.* **1995**, *99*, 15269.
(15) Manner, W. L.; Bishop, A. R.; Girolami, G. S.; Nuzzo, R. G. *J. Phys. Chem.* **1998**, *102*, 8816.
(16) Fuhrmann, D.; Wöll, Ch. *Surf. Sci.* **1997**, *377*−379, 544.
(17) Porter, M. D.; Bright, T. B.; Allara, D. L.; Chidsey, C. F. D. *J. Am. Chem. Soc.* **1987**, *109*, 3559.
(18) Walczak, M. M.; Cung, C.; Stole, S. M.; Widrig, C. A.; Porter, M. D. *J. Am. Chem. Soc.* **1991**, *113*, 2370.
(19) Laibinis, P. E.; Whitesides, G. M.; Allara, D. L.; Tao, Y.; Parikh, A. N.; Nuzzo, R. G. *J. Am. Chem. Soc.* **1991**, *113*, 7152.
(20) Nuzzo, R. G.; Korenic, E. M.; Dubois, L. H. *J. Chem. Phys.* **1990**, *93*, 767.
(21) Badia, A.; Cuccia, L.; Demers, L.; Morin, F.; Lennox, R. B. *J. Am. Chem. Soc.* **1997**, *119*, 2682.
(22) Teuscher, J. H.; Yeager, L. J.; Yoo, H.; Chadwick, J. E.; Garrell, R. L. *Faraday Discuss.* **1997**, *107*, 399.
(23) Allara, D. L.; Nuzzo, R. G. *Langmuir* **1985**, *1*, 45.
(24) Allara, D. L.; Nuzzo, R. G. *Langmuir* **1985**, *1*, 52.
(25) Tao, Y. *J. Am. Chem. Soc.* **1993**, *115*, 4350.
(26) Samant, M. G.; Brown, C. A.; Gordon, J. G. *Langmuir* **1993**, *9*, 1082.
(27) Theng, B. K. G. *The Chemistry of Clay-Organic Reactions*; Adam Hilger: London, 1974.
(28) *Tonminerale und Tone*; Jasmund, K., Lagaly, G., Eds.; Steinkopf: Darmstadt, 1993; p 6, 140, 145.
(29) Weiss, A. *Angew. Chem., Int. Ed. Engl.* **1963**, *2*, 134.
(30) Lagaly, G.; Weiss, A. *Kolloid-Z.* **1971**, *248*, 968.
(31) Lagaly, G. *Angew. Chem., Int. Ed. Engl.* **1976**, *15*, 575
(32) Lagaly, G. *Philos. Trans. R. Soc. London, Ser. A* **1984**, *311*, 315.
(33) Lagaly, G. *Solid State Ionics* **1986**, *22*, 43.
(34) Vaia, R. A.; Teukolsky, R. K.; Giannelis, E. P. *Chem. Mater.* **1994**, *6*, 1017.
(35) Newman, A. C. D.; Brown, G. In *Chemistry of Clays and Clay Minerals*; Newman, A. C. D., Ed.; Longman: Essex, 1987; p 59.
(36) Lagaly, G. *Clay Miner. Soc. Workshop Lect.* **1994**, *6*, 1.
(37) Osman, M. A.; Suter, U. W. *J. Colloid Interface Sci.* **1999**, *214*, 400.
(38) Meier, L. P.; Shelden, R. A.; Caseri, W. R.; Suter, U. W. *Macromolecules* **1994**, *27*, 1637.
(39) Geke, M. O.; Shelden, R. A.; Caseri, W. R.; Suter, U. W. *J. Colloid Interface Sci.* **1997**, *189*, 283.
(40) Velten, U.; Shelden, R. A.; Caseri, W. R.; Suter, U. W.; Yuzhuo, Li *Macromolecules* **1999**, *32*, 3590.
(41) Osman, M. A.; Moor, C.; Caseri, W. R.; Suter, U. W. *J. Colloid Interface Sci.* **1999**, *209*, 232.
(42) Osman, M. A.; Caseri, W. R.; Suter, U. W. *J. Colloid Interface Sci.* **1998**, *198*, 157.
(43) Lin-Vien, D.; Colthup, N. B.; Fateley, W. G.; Grasselli, J. G. *The Handbook of Infrared and Raman Characteristic Frequencies of Organic Molecules*; Academic Press: San Diego, 1991; p 11.
(44) Dubois, L. H.; Nuzzo, R. G.; Allara, D. L. *J. Am. Chem. Soc.* **1990**, *112*, 558.
(45) Snyder, R. G.; Hsu, S. L.; Krimm, S. *Spectrochim. Acta, Part A* **1978**, *34*, 395.
(46) Snyder, R. G.; Strauss, H. L.; Elliger, C. A. *J. Phys. Chem.* **1982**, *86*, 5145.
(47) MacPhail, R. A.; Strauss, H. L.; Snyder, R. G.; Elliger, C. A. *J. Phys. Chem.* **1982**, *88*, 334.
(48) Maroncelli, M.; Qi, S. P.; Strauss, H. L.; Snyder, R. G. *J. Am. Chem. Soc.* **1982**, *104*, 6237.
(49) Snyder, R. G.; Maroncelli, M.; Strauss, H. L.; Hallmark, V. M. *J. Phys. Chem.* **1986**, *90*, 5623.
(50) Parikh, A. N.; Schivley, M. A.; Koo, E.; Seshadri, K.; Aurentz, D.; Mueller, K.; Allara, D. L. *J. Am. Chem. Soc.* **1997**, *119*, 3135.
(51) Guzonas, D. A.; Hair, M. L.; Tripp, C. P. In *Fourier Transform Infrared Spectroscopy in Colloid and Interface Science*; Scheuing, D. R., Ed.; ACS Symposium Series 447; American Chemical Society: Washington, DC, 1998; p 237.
(52) Bailey, S. W. In *Crystal Structures of Clay Minerals and Their X-Ray Identification*; Brindley, G. W., Brown, G., Eds.; Mineralogical Society: London, 1980; p 62.